Structure-Based Optimization of the Terminal Tripeptide in Glycopeptide Dendrimer Inhibitors of Pseudomon....

Article *in* Chemistry - A European Journal · December 2013

DOI: 10.1002/chem.201302587 · Source: PubMed

CITATIONS
25

READS
72

7 authors, including:

Rameshwar U. Kadam
The Scripps Research Institute
30 PUBLICATIONS **753** CITATIONS
SEE PROFILE

Myriam Bergmann
Universität Bern
7 PUBLICATIONS **194** CITATIONS
SEE PROFILE

Achim Stocker
Universität Bern
73 PUBLICATIONS **1,973** CITATIONS
SEE PROFILE

Tamis Darbre
Universität Bern
116 PUBLICATIONS **2,979** CITATIONS
SEE PROFILE

CHEMISTRY
A EUROPEAN JOURNAL

ChemPubSoc
Europe

DOI: 10.1002/chem.201302587

Structure-Based Optimization of the Terminal Tripeptide in Glycopeptide Dendrimer Inhibitors of *Pseudomonas aeruginosa* Biofilms Targeting LecA

Rameshwar U. Kadam,[a] Myriam Bergmann,[a] Divita Garg,[b] Gabriele Gabrieli,[a] Achim Stocker,[a] Tamis Darbre,[a] and Jean-Louis Reymond*[a]

Abstract: The galactopeptide dendrimer **GalAG2** ((β-Gal-OC_6H_4CO-Lys-Pro-Leu)$_4$(*Lys*-Phe-Lys-Ile)$_2$*Lys*-His-Ile-NH_2) binds strongly to the *Pseudomonas aeruginosa* (PA) lectin LecA, and it inhibits PA biofilms, as well as disperses already established ones. By starting with the crystal structure of the terminal tripeptide moiety **GalA-KPL** in complex with LecA, a computational mutagenesis study was carried out on the galactotripeptide to optimize the peptide–lectin interactions. 25 mutants were experimentally evaluated by a hemagglutination inhibition assay, 17 by isothermal titration calorimetry, and 3 by X-ray crystallography. Two of these tripeptides, **GalA-KPY** (dissociation constant (K_D) = 2.7 μM) and **GalA-KRL** (K_D = 2.7 μM), are among the most potent monovalent LecA ligands reported to date. Dendrimers based on these tripeptide ligands showed improved PA biofilm inhibition and dispersal compared to those of **GalAG2**, particularly **G2KPY** ((β-Gal-OC_6H_4CO-Lys-Pro-Tyr)$_4$(*Lys*-Phe-Lys-Ile)$_2$-*Lys*-His-Ile-NH_2). The possibility to retain and even improve the biofilm inhibition in several analogues of **GalAG2** suggests that it should be possible to fine-tune this dendrimer towards therapeutic use by adjusting the pharmacokinetic parameters in addition to the biofilm inhibition through amino acid substitutions.

Keywords: biofilms · dendrimers · glycopeptides · inhibition · proteins

Introduction

The rise of antibiotic-resistant bacteria is one of the major healthcare problems today. In the case of the opportunistic human pathogen *Pseudomonas aeruginosa*, antibiotic resistance is associated with biofilm formation in airway infections, and this is lethal for immunocompromised and cystic fibrosis patients in many cases.[1] One possible life-saving strategy consists of developing biofilm inhibitors so as to restore antibiotic sensitivity without inducing a resistance phenomenon.[2] Tissue attachment and biofilm formation in *P. aeruginosa* is mediated in part by the galactose-specific lectin LecA[3] and the fucose-specific lectin LecB.[4] The crucial in vivo role of lectins is evidenced by impaired biofilm formation in deletion mutants[5] and by the successful treatment of *P. aeruginosa* infections with concentrated carbohydrate solutions.[2a,6] LecA and LecB are tetrameric proteins with four identical carbohydrate-binding sites.[7] They are believed to act as cross-linking agents by binding to cell-surface glycosides, which has led to the hypothesis that inhibitors of such lectins might also suppress biofilms. Various synthetic inhibitors of LecA,[8] LecB,[9] or both[10] have been reported that feature multiple glycosides displayed on a multivalent scaffold[11] to follow the principle of the cluster glycoside effect.[12] We recently reported such lectin inhibitors in the form of glycopeptide dendrimers[13] displaying four fucosides (**FD2**)[14] or four galactosides (**GalAG2** and **GalBG2**)[15] at the end of a common peptide dendrimer scaffold (Figure 1 A).[16] These dendrimers bind tightly to their respective lectins and represent the only multivalent systems to date with documented inhibitory activity on *P. aeruginosa* biofilms.

The amino acid sequence of our peptide dendrimer biofilm inhibitors was initially identified in a combinatorial binding assay[17] of a fucosylated peptide dendrimer library towards the fucose-specific plant lectin UEA-I.[18] This led to dendrimer **FD2**, which also strongly inhibited LecB and blocked the formation and induced the dispersion of *P. aeruginosa* biofilms. Amino acid sequence variations were investigated for the fucosylated dendrimer **FD2** and were found to modulate the lectin-binding affinity, dendrimer solubility, and biofilm inhibition.[19] The crystal structure of the complex between LecB and the terminal fucosylated tripeptide **FD0**, however, showed a disordered tripeptide without significant contacts to the lectin.[14] A similarly disordered tri-

[a] Dr. R. U. Kadam,[+] M. Bergmann,[+] G. Gabrieli, Dr. A. Stocker, Dr. T. Darbre, Prof. Dr. J.-L. Reymond
Department of Chemistry and Biochemistry
University of Berne
Freiestrasse 3, 3012 Berne (Switzerland)
Fax: (+41) 31-631-80-57
E-mail: jean-louis.reymond@ioc.unibe.ch

[b] Dr. D. Garg
Institute of Structural Biology, Helmholtz Zentrum München
and Center for Integrated Protein Science Munich at Dept. Chemie
Technische Universität München
Lichtenbergstrasse 4, 85747 Garching (Germany)

[+] These authors contributed equally to the work.

Supporting information for this article is available on the WWW under http://dx.doi.org/10.1002/chem.201302587.

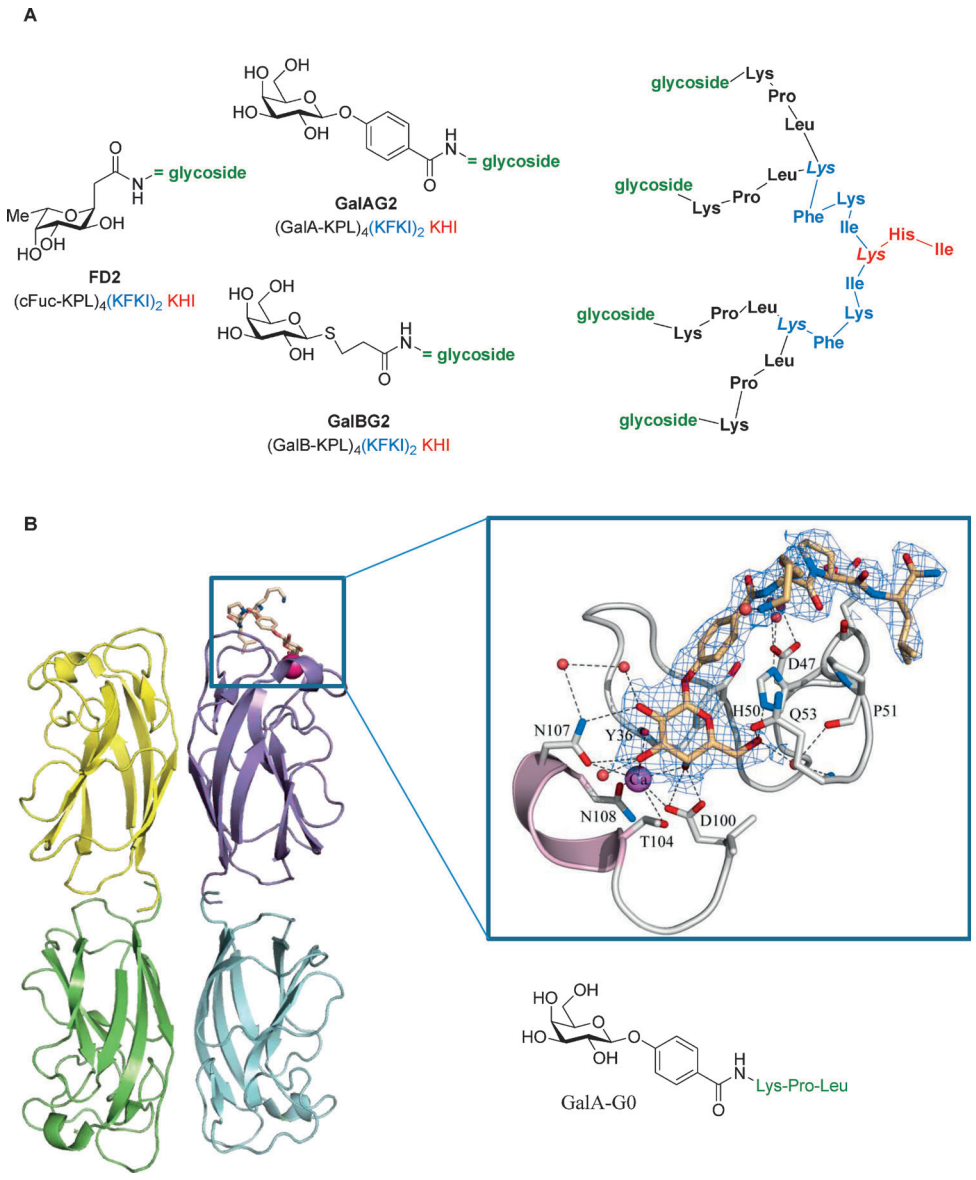

Figure 1. Structure of glycopeptide dendrimer biofilm inhibitors. A) Structure diagram. One-letter codes are used for L-amino acids in the abbreviated nomenclature. Branching lysine residues are indicated by italics. The C terminus is at the core of the dendrimer as a carboxamide group ($CONH_2$). B) Crystal structure of the **GalAG0**–LecA complex. Inset: Close-up view of the LecA glycopeptide-binding site.

peptide structure was observed in the complex of the weakly binding tripeptide **GalBG0** with LecA.[15]

In the case of the **GalAG0**–LecA complex, by contrast, the terminal tripeptide was well resolved due to the strong binding between the aromatic group of the galactoside and LecA, which involved an unusual CH–π T-shaped interaction to the C(ε1)-H group of residue H50.[15,20] This interaction was reflected in the much stronger binding affinities of the aromatic glycoside **GalA**-type ligands to LecA relative to those of the aliphatic thioglycoside **GalB**-type ligands. Despite the well-resolved tripeptide portion of **GalAG0**–LecA, there were only a few contact points between the amino acids and the protein, which suggested that mutagenesis might improve the binding (Figure 1B). We therefore set out to investigate amino acid substitutions in **GalAG2** as a strategy to increase LecA binding and biofilm inhibition.

Herein, we report an amino acid sequence variation study that shows the role of individual residues in the activity of **GalAG2**. After an initial alanine scan to highlight the critical role of the terminal tripeptide for activity, a structure-based drug-design effort was undertaken to optimize the binding interactions between the terminal galactotripeptide **GalAG0** and the lectin. 101 different tripeptide sequence variants were evaluated by docking, of which 25 were synthesized and tested for binding to LecA by a hemagglutination inhibition assay, 17 were analysed by isothermal titration calorimetry, and 3 were investigated by X-ray crystallography of the galactotripeptide–LecA complexes. Two of these tripeptides, **GalA-KPY** (dissociation constant (K_D) = 2.7 μM) and **GalA-KRL** (K_D = 2.7 μM), are among the most potent monovalent LecA ligands reported to date. Although the monovalent galactotripeptides did not inhibit biofilms, incorporation of the selected tripeptide sequences into the **GalAG2** dendrimer led to new dendrimers with stronger biofilm inhibition and dispersal effects, particularly **G2KPY** ((β-Gal-OC_6H_4CO-Lys-Pro-Tyr)$_4$(*Lys*-Phe-Lys-Ile)$_2$*Lys*-His-Ile-NH_2). This study delineates the details of the structure–activity landscape of peptide dendrimer **GalAG2** as a potent LecA ligand and *P. aeruginosa* biofilm inhibitor. The possibility to retain and even improve biofilm inhibition in several analogues of **GalAG2** suggests that it should be possible to fine-tune this dendrimer towards therapeutic use by adjusting the pharmacokinetic parameters in addition to the biofilm inhibition through amino acid substitutions.

Results and Discussion

Alanine scan: To gain a first insight into which amino acid position most affected the activity of **GalAG2**, each of the non-branching amino acids was substituted by alanine. The eight dendrimers were prepared by solid-phase peptide synthesis (SPPS) with 9-fluorenylmethoxycarbonyl (Fmoc) protection on Rink-amide resin (0.3 mmol g^{-1}). The N terminus was capped with 4-(tetra-*O*-acetyl-β-D-galactopyranosyloxy)benzoic acid (**AcGalA-OH**),[15] and this was followed by on-resin deacetylation by treatment with methanolic ammonia. The galactosylated peptide dendrimers were obtained as pure products after cleavage from the resin and side-chain deprotection by treatment with trifluoroacetic acid (TFA) in the presence of triisopropylsilane (TIS) and water as scavengers, precipitation from diethyl ether, and purification by preparative reversed-phase HPLC (Scheme 1, Table 1).

In terms of the physico-chemical properties, the Ala-scan mutants were very similar to the parent dendrimer **GalAG2**. In particular, the alanine mutations did not affect the water solubility of **GalAG2** except for **Ala-4**, in which the replacement of the lysine residue in the first-generation branch reduced the water solubility, so a dimethylsulfoxide (DMSO) stock solution had to be prepared in this case.

Binding to LecA was evaluated by the hemagglutination inhibition assay (HIA), which indicated that the alanine-scan dendrimers and the parent **GalAG2** bound LecA comparably well and gave comparable MIC values within one dilution, values that correspond to 1000-fold stronger inhibition of LecA-induced hemagglutination than that by D-galactose. The effect of the Ala-scan mutants on the inhibition and dispersion of *P. aeruginosa* biofilms by **GalAG2** was more pronounced. Biofilms were measured in a microtiter plate by using a modified version of a previously reported assay[5c] with phenazine ethosulfate and the formazan dye precursor 2-(2-methoxy-4-nitrophenyl)-3-(4-nitrophenyl)-5-(2,4-disulfophenyl)-2*H*-tetrazolium (WST-8) to detect live bacteria in the surface-attached biofilm. WST-8 forms a water-soluble formazan, which allows for a better quantification of live bacteria than 3-(4,5-dimethylthiazol-2-yl)-2,5-diphenyltetrazolium bromide (MTT).[21] The biofilm assay was calibrated by reproducing biofilm inhibition and dispersion data obtained earlier[14,15] by using the steel-coupon assay[22] with dendrimers **FD2**, **GalAG2**, and **GalBG2**, with the advantage that the 96-well microtiter-plate format consumed much smaller amounts of compound.

Biofilm inhibition was either unaffected or reduced twofold by the alanine substitutions with the exception of **Ala-8**, which did not show any biofilm inhibitory activity in the measured concentration range, a result that highlights the critical role of the residues next to the galactose. On the other hand, the biofilm dispersion effect was only affected by substitutions near the core, in **Ala-3**, **Ala-2**, and **Ala-1**, which highlights the additional effects of the peptide dendrimer portion of **GalAG2** on its activity.

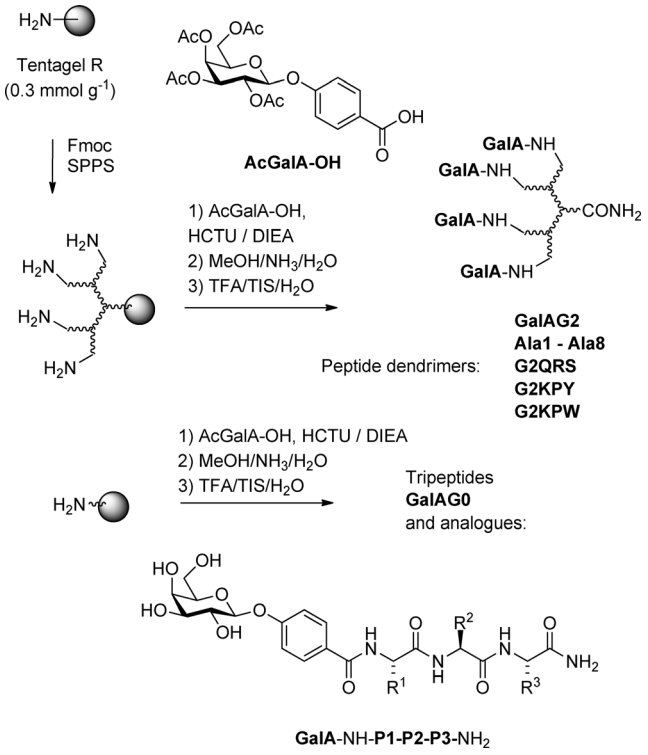

Scheme 1. SPPS of galactosylated peptide dendrimers and tripeptides. HCTU: *O*-(1*H*-6-chlorobenzotriazol-1-yl)-1,1,3,3-tetramethyluronium hexafluorophosphate; DIEA: *N*,*N*-diisopropylethylamine.

Table 1. Synthesis and evaluation of the alanine-scan series.

Compound	Sequence[a]	Mass ion calcd/obs	Yield [mg] ([%])	MIC[b] [μM]	MBIC[c] [μM]	Disp.[d] [%]
D-Gal	D-galactose	–	–	6250	–	–
GalAG2	(GalA-KPL)$_4$(*K*FKI)$_2$*K*HI	3911.6/3911	42 (7)	1.56	20	40
Ala-8	(GalA-APL)$_4$(*K*FKI)$_2$*K*HI	3683.2/3682.9	11 (4)	1.56	>45	40
Ala-7	(GalA-KAL)$_4$(*K*FKI)$_2$*K*HI	3807.5/3807	22 (8)	1.56	13	50
Ala-6	(GalA-KPA)$_4$(*K*FKI)$_2$*K*HI	3743.3/3743	23 (9)	0.78	30	50
Ala-5	(GalA-KPL)$_4$(*K*AKI)$_2$*K*HI	3759.4/3759	36 (13)	0.78	45	20
Ala-4	(GalA-KPL)$_4$(*K*FAI)$_2$*K*HI	3797.4/3797.2	9 (3)	0.78	45	65
Ala-3	(GalA-KPL)$_4$(*K*FKA)$_2$*K*HI	3827.5/3726	17 (6)	0.78	45	n.a.
Ala-2	(GalA-KPL)$_4$(*K*FKI)$_2$*K*AI	3845.5/3844	17 (6)	0.78	20	10
Ala-1	(GalA-KPL)$_4$(*K*FKI)$_2$*K*HA	3869.5/3869	34.5 (12)	0.78	30	n.a.

[a] Single letter codes for L-amino acids; branching lysine residues indicated by italics; GalA is 4-(β-galactosyloxy)benzoyl; the peptide C terminus is a carboxamide $CONH_2$ group. [b] MIC: minimum inhibition concentration in the hemagglutination assay with rabbit erythrocytes. See the Materials and Methods section for details. [c] MBIC: minimum biofilm inhibition concentration. See the Materials and Methods for details. [d] Dispersal at 50 μM dendrimer concentration. n.a.: not active. See also Figure S69 and S71a in the Supporting Information.

Overall, the effect of alanine substitutions in **GalAG2** on the lectin binding and biofilm inhibition activity was interpreted as a basis to undertake a mutagenesis study focusing on the terminal tripeptide, with the fact that this tripeptide occurs in four copies in the dendrimer and makes direct contact with the lectin also taken into account.

Docking selection of GalAG0 mutants: The tripeptide **GalAG0**, which corresponds to the outermost branch in **GalAG2**, is well resolved in the crystal structure of its complex with LecA (Figure 1B). The structure shows that there are few contact points between the peptide and the protein, which suggests that mutagenesis might be used to increase the binding. A docking study was undertaken to select tripeptide mutants of **GalAG0** for synthesis and testing. Docking was performed with the docking program Glide, which correctly positioned the reference tripeptide **GalAG0** in its crystallographically determined pose (see Materials and Methods section).

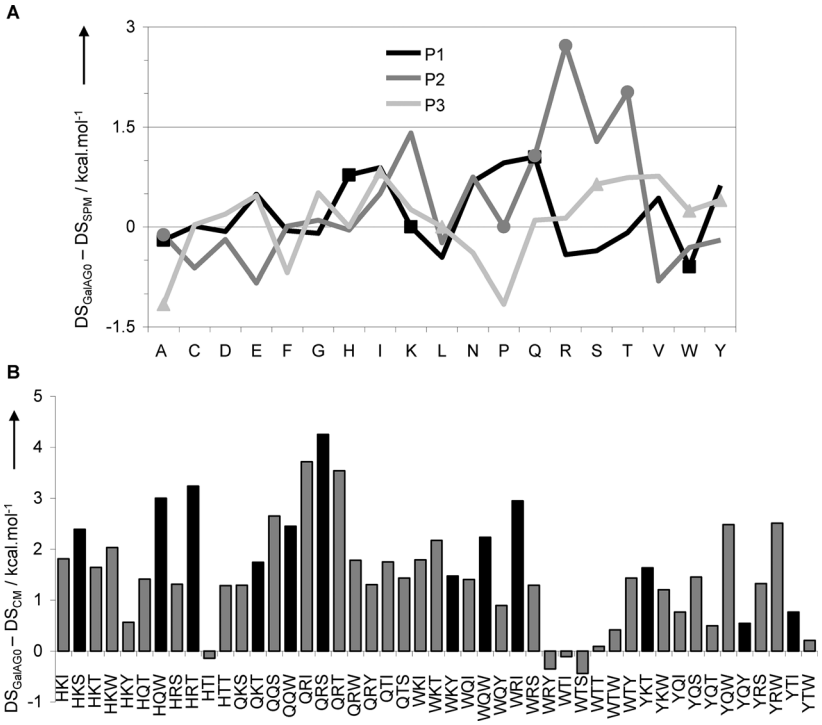

Figure 2. Increase in docking score (DS) to LecA for galactosylated tripeptides GalA-P1P2P3 relative to **GalAG0** (GalA-KPL). A) SPM analogues of **GalAG0**. Experimentally evaluated compounds have visible data-point labels. B) CM analogues of **GalAG0**. Experimentally evaluated compounds have black bars. The difference in the Glide score relative to the score of **GalAG0** is plotted as a function of the tripeptide sequence (higher values = stronger). Docking score values are listed in Tables S2 and S3 in the Supporting Information.

A series of 54 single-point mutants (SPMs) of **GalAG0** was investigated first. For all of the docked tripeptides, the galactosyl group occupied the galactose-binding pocket, the aromatic glycosidic group engaged in a CH–π T-shaped interaction with the C(ε1)-H group of residue H50, and the amino acids engaged in various interactions with the loop D47–Q53 in LecA. Mutation of the P1 lysine into charged or polar residues, such as glutamic acid, aspartic acid, glutamine, asparagine, or tyrosine, gave good docking scores, mostly due to H-bond formation with $Q53_{LecA}$. Similarly, positively charged and polar amino acid mutants of the P2-proline, for example, lysine, arginine, histidine, and tryptophan mutants, engaged in H-bonding with the side chain of E49, whereas the side chain of the threonine mutant H-bonded with the E49 backbone, which resulted in a higher docking score. Mutation of the P3 leucine to tryptophan or tyrosine resulted in improved hydrophobic contacts with LecA and, in the case of tryptophan, in the formation of an additional H-bond with the backbone of R48. On the other hand, mutations of the P3 leucine to cysteine or glutamine resulted in an altered side-chain orientation that allowed H-bonding with E49 and increased docking scores (Figure 2A).

In the computational approach, a further 47 combined mutants (CMs) were investigated by the combination of several of the residues associated with favourable docking scores in the SPM series. Furthermore, tryptophan was introduced at P1 and P3 to account for the fact that tryptophan often increases peptide–protein binding by offering a large aromatic and at the same time hydrophobic surface area. The CM series yielded significantly increased docking scores relative to those of the SPM series (Figure 2B).

Experimental evaluation of GalAG0 mutants: Thirteen SPM and twelve CM analogues of **GalAG0** were selected from the docking study and prepared by SPPS with Fmoc protection by using the same procedure as that used for the dendrimers, with capping of the N terminus with 4-(tetra-*O*-acetyl-β-D-galactopyranosyloxy)benzoic acid (**AcGalAOH**; Scheme 1). On-resin deacetylation by treatment with methanolic ammonia, acidic cleavage from the resin and side-chain deprotection, precipitation from diethyl ether, and purification by preparative reversed-phase HPLC gave the galactosylated tripeptides as pure products in good yields (Table 2).

All of the tripeptides were evaluated for binding to LecA by an HIA. The tripeptides inhibited LecA-induced hemagglutination 10–80 times more strongly than D-galactose, with the strongest binding observed for tripeptides containing an aromatic residue at P1 (**GalA-WPL**, **GalA-WKY**, **GalA-**

Table 2. Synthesis and evaluation of galactosylated tripeptides for binding to LecA.

Sequence[a]	Mass ion calcd/obs	Yield [mg] ([%])	MIC[b] [μM]	Isothermal titration calorimetry (ITC)[c] ΔH [kcal mol^{-1}]	$-T\Delta S$ [kcal mol^{-1}]	K_D [μM]	r.p.[d]
GalA-KPL	638.7/638.4	51 (72)	312	−10.8 ± 0.7	3.4 ± 0.8	4.3 ± 0.1	20
GalA-APL[e]	581.27/581.28	31.5 (49)	625	−7.7	1.1	14.7	6
GalA-HPL	647.7/647.4	47 (66)	625			–	–
GalA-QPL	638.3/638.3	27.7 (39)	625			–	–
GalA-WPL	694.8/694.4	52 (68)	156	−10.6 ± 0.5	3.6 ± 1.5	7.4 ± 0.3	12
GalA-KAL[e]	612.7/612.6	12.4 (18)	625	−10.2	3.2	7.3	12
GalA-KQL	669.7/669.2	43.5 (59)	625			–	–
GalA-KRL	696.8/697	26.8 (35)	156	−12.8 ± 0.4	5.2 ± 0.5	2.7 ± 0.3	33
GalA-KTL	642.7/642.2	35 (50)	625			–	–
GalA-KPA[e]	596.6/596.2	36.4 (56)	312	−9.8	2.8	7.9	11
GalA-KPI	638.7/639.4	17.4 (25)	625	−12.1 ± 0.1	4.8 ± 0.1	4.6 ± 0.1	19
GalA-KPS[e]	612.6/612.2	26.8 (40)	625	−12.7	5.3	4.3	20
GalA-KPW	711.8/711.4	6.2 (8)	156	−12.5 ± 0.3	5.3 ± 0.3	5.2 ± 0.6	17
GalA-KPY	688.7/688.4	19.7 (26)	312	−15.0 ± 0.3	7.4 ± 0.2	2.7 ± 0.5	33
GalA-HKS	652.7/652.4	42 (58)	625			–	–
GalA-HQW	751.75/751.4	6.7 (8)	312	−10.8 ± 0.5	3.7 ± 0.5	6.1 ± 0.8	14
GalA-HRT	694.3/694.3	20.8 (27)	78	−12.5 ± 0.1	5.5 ± 0.2	6.9 ± 0.3	13
GalA-QKT	657.7/657.4	51.3 (71)	625			–	–
GalA-QQW	742.7/742.2	30.6 (38)	625			–	–
GalA-QRS	671.7/671.4	16.9 (23)	625	−12.0 ± 0.3	4.7 ± 0.4	4.5 ± 0.5	20
GalA-WKY	777.8/777.4	15.4 (18)	78	−8.0 ± 0.5	0.7 ± 0.7	4.3 ± 1.1	20
GalAWQW	800.32/800.32	6.8 (8)	78			–	–
GalA-WRI	755.8/755.4	6.7 (8)	78	−11.2 ± 0	3.8 ± 0	4.3 ± 0.2	20
GalA-YKT	692.7/692.4	53.9 (71)	156	−12.8 ± 0.1	5.3 ± 0.1	3.2 ± 0.1	28
GalA-YQW	777.8/777.4	18.9 (22)	156			–	–
GalA-YRW	805.9/805.4	12.8 (14)	78	−11.7 ± 0.1	4.4 ± 0.3	4.6 ± 1.0	19

[a] Single letter codes for L-amino acids; GalA is 4-(β-galactosyloxy)benzoyl; the peptide C terminus is a carboxamide $CONH_2$ group. [b] MIC: minimum inhibition concentration in the hemagglutination assay with rabbit erythrocytes. See the Materials and Methods section for details. The MIC value for galactose is 6.25 mM. [c] Thermodynamic parameters and dissociation constants (K_D) reported as an average of two independent runs (unless stated otherwise) from ITC in 0.1 M tris(hydroxymethyl)aminomethane (Tris)–base (pH 7.5) with 25 mM $CaCl_2$ at 25 °C. [d] r.p.: relative potency compared to D-galactose, calculated as r.p. = K_D(galactose)/K_D(compound). The K_D value for galactose is (88 ± 4) μM. [e] K_d values reported as a single run from ITC. The stoichiometry (n) in all cases was set to one. The ITC experiments were conducted at c values of 3–15, which generates accurate ΔH and K_D values with known stoichiometry and saturation, as was the case here.[23]

WRI, **GalA-YRW**). The better binders were further evaluated by isothermal titration calorimetry (ITC), which yielded dissociation constants in the relatively narrow range of 2.7 μM < K_D < 14.7 μM; however, the values were not correlated with the MIC values or the presence of an aromatic residue. Nevertheless, several galactosylated tripeptides showed stronger binding affinity than the reference ligand **GalAG0**. In particular, **GalA-KPY** and **GalA-KRL** represent the most potent monovalent GalA ligands reported to date.[8e]

Strong binding correlated with strongly negative binding enthalpies and a high entropy penalty. The effect was most pronounced in **GalA-KPY** ($\Delta H = -15$ kcal mol^{-1}; $-T\Delta S = +7.4$ kcal mol^{-1}) and can be interpreted in terms of enthalpically favourable contacts between the conformationally flexible tripeptide portion of the ligand and LecA inducing entropically unfavourable immobilization. Conversely, there was almost no entropy change upon binding of **GalA-WKY** to LecA. This suggests few peptide–protein contacts in this case, which is consistent with the observed binding mode in the LecA–**GalA-WKY** crystal structure (see below).

Structural characterization of ligand–LecA complexes: All of the tripeptides were subjected to crystallization screening in their complex with LecA. Crystal structures of LecA–tripeptide complexes were successfully obtained with the three tripeptides **GalA-QRS**, **GalA-WRI**, and **GalA-WKY** (Table 3). In all three cases, the galactose bound in the expected galactose-binding site and the phenyl aglycone engaged in a T-shaped interaction with $H50_{LecA}$, as previously observed in the **GalAG0**–LecA complex (Figure 3A and B).[15] However, the tripeptide portions of the ligands were flexible and adopted alternative conformations. In the case of **GalA-QRS**, the asymmetric unit contained eight LecA monomers and eight independent galactose-binding sites, four of which contained well-resolved ligands displaying four different conformations (Figure S74 in the Supporting Information). One of these conformations matched the computational docking pose of **GalA-QRS** with an atom-pairwise root mean square (RMS) value of 2.47 Å and reproduced key predicted docking interactions, such as the side-chain hydrophobic contacts of $Q1_{\mathbf{GalA\text{-}QRS}}$ with $P51_{LecA}$, the salt bridge between $R2_{\mathbf{GalA\text{-}QRS}}$ and $E49_{LecA}$, and the water-mediated H-bond between $R2_{\mathbf{GalA\text{-}QRS}}$ and $H50_{LecA}$. On the other hand, the predicted H-bonds of $S3_{\mathbf{GalA\text{-}QRS}}$ with the backbone carbonyl groups of $E49_{LecA}$ and $H50_{LecA}$ were not observed because this residue was found to be fully solvent exposed (Figure 3C and F).

The co-crystal structure of **GalA-WRI** (or, respectively, **GalA-WKY**) contained four (two) independent galactose-binding sites, two (one) of which were fully occupied by the ligand and featured two (one) tripeptide structure (Figure 3D and E). In both structures, the hydrophobic aromatic residues of the tripeptide engaged in crystal contacts toward neighbouring crystal units (Figure S75 and S76 in the Supporting Information) and therefore did not match the predicted docking contacts ($I3_{\mathbf{GalA\text{-}WRI}}$ and $W1_{\mathbf{GalA\text{-}WKY}}$ to $P53_{LecA}$, $Y3_{\mathbf{GalA\text{-}WKY}}$ to $P38_{LecA}$, $Q40_{LecA}$, and $W42_{LecA}$; Figure 3G and H). Overall, the diversity of experimental poses observed for the tripeptides showed that the GalA-tripeptide–LecA contacts were generally weak, which might ex-

Table 3. Data collection and refinement statistics.

	GalA-QRS–LecA	GalA-WRI–LecA	GalA-WKY–LecA
beam line	PSI PX III	PSI PX III	PSI PX III
wavelength [Å]	1.00000	1.00000	1.00000
resolution [Å]	48.46–2.31 (2.45–2.31)[a]	44.11–1.65 (1.75–1.65)[a]	46.78–1.64 (1.74–1.64)[a]
Cell dimensions			
space group	$C2$	$P2_12_12_1$	$P4_322$
unit cell [Å]	$a=158.8$, $b=148.6$, $c=86.7$ $\alpha=\gamma=90°$, $\beta=110.8°$	$a=60.9$, $b=64.5$, $c=155.6$ $\alpha=\beta=\gamma=90°$	$a=95.3$, $b=95.3$, $c=107.3$ $\alpha=\beta=\gamma=90°$
measured/unique reflections	200722/81750	264603/72701	426261/112785
average multiplicity	2.4 (2.3)[a]	3.6 (3.6)[a]	3.7 (3.6)[a]
completeness [%]	98.0 (92.9)[a]	98.7 (95.0)[a]	97.1 (93.3)[a]
average $I/\sigma(I)$	9.14 (2.0)[a]	10.94 (2.34)[a]	21.22 (2.96)[a]
R_{merge} [%]	19.5 (78.9)[a]	17.9(89.8)[a]	8.8 (54.3)[a]
Wilson B-factor	33.6	23.2	25.6
Refinement			
resolution range [Å]	49.26–2.31	44.11–1.65	46.78–1.64
R_{work} [%]	21.46	20.41	19.23
R_{free} [%]	24.74	22.30	21.27
average Biso [Å^2]			
all atoms	35.03	28.68	27.53
protein atoms	27.51	21.26	19.41
glycopeptide atoms	42.30	30.96	30.68
solvent atoms	35.29	33.84	32.51
RMS deviation from ideality angles [°]	0.672	1.047	1.061
bonds [Å]	0.002	0.007	0.006
water molecules	1157	706	433
number of galactose	8	4	2
calcium atoms	8	4	2
Protein Data Bank deposition code	4LKD	4LKE	4LKF

[a] Values in parentheses correspond to the highest resolution shell.

plain the relatively narrow range of LecA binding affinities observed among the different tripeptides tested, including the lack of affinity increase in tripeptides bearing large aromatic and hydrophobic residues, as well as the poor predictive power of the docking selection.

Inhibition and dispersal of *P. aeruginosa* biofilms: As was previously observed with **GalAG0**, none of the 25 synthesized galactotripeptides showed any significant inhibition of *P. aeruginosa* biofilm formation, a result that is in line with our previous observation that multivalency is critical for biofilm inhibition by LecA inhibitors.[15] The G2 dendrimers corresponding to five of the more potent galactotripeptides, including the three examples for which a LecA co-crystal structure had been obtained, were prepared by SPPS. Although the dendrimer synthesis with the sequences derived from the relatively hydrophobic tripeptides **GalA-WRI** and **GalA-WKY** gave intractable insoluble products, three peptide dendrimers were obtained in good yields and purity, namely, **G2QRS**, **G2KPY**, and **G2KPW** (Table 4).

LecA binding was evaluated by a hemagglutination assay, which showed that these three dendrimers bound LecA with comparable strength to **GalAG2**. Most importantly, all three dendrimers displaying the galactotripeptide in tetravalent mode showed good biofilm inhibition and dispersion effects. In terms of biofilm inhibition, **G2QRS** and **G2KPY** were slightly weaker biofilm inhibitors than **GalAG2**, whereas **G2KPW** was as potent as **GalAG2**. The most striking difference occurred in the biofilm dispersal assay, which showed that **G2KPY** and **G2KPW** were both significantly better for biofilm dispersal than **GalAG2** or **G2QRS**. With LecA binding, biofilm inhibition, and biofilm dispersal data taken into account, dendrimer **G2KPY** appears to be the best ligand so far.

Conclusion

The experiments described above document the influence of amino acid exchanges on the LecA binding and *P. aeruginosa* biofilm inhibition and dispersal properties of the galactopeptide dendrimer **GalAG2**. The alanine scan showed that LecA binding, biofilm inhibition, and biofilm dispersal most critically depend on the properties of the terminal galactosylated tripeptide that is present in four copies and is in direct contact with the lectin. The structure-based drug-design effort allowed a moderate improvement in the binding from $K_D=(4.3\pm0.1)$ μM in the starting ligand **GalA-KPL** (**GalAG0**) to $K_D=(2.7\pm0.5)$ μM in **GalA-KRL** and **GalA-KPY**. These tripeptides belong to the most potent monovalent inhibitors reported to date for the *P. aeruginosa* lectin LecA. The best tripeptides in terms of LecA binding were SPM variations of the original KPL sequence that retained one cationic residue and one hydrophobic residue. A combination of these features in the tripeptide moiety seems to be optimal for binding to LecA. None of the monovalent galactotripeptides showed any effect on biofilm inhibition or dispersal. However, the introduction of the KPY and KPW sequences into the tetravalent dendrimers **G2KPY** and **G2KPW** gave good biofilm inhibitors with similar affinity for LecA to that of **GalA-G2**, but with higher ability to disperse biofilms. These results further confirm our previous findings that multivalency is essential for biofilm inhibition and show that this bioactivity is sensitive to the amino acid

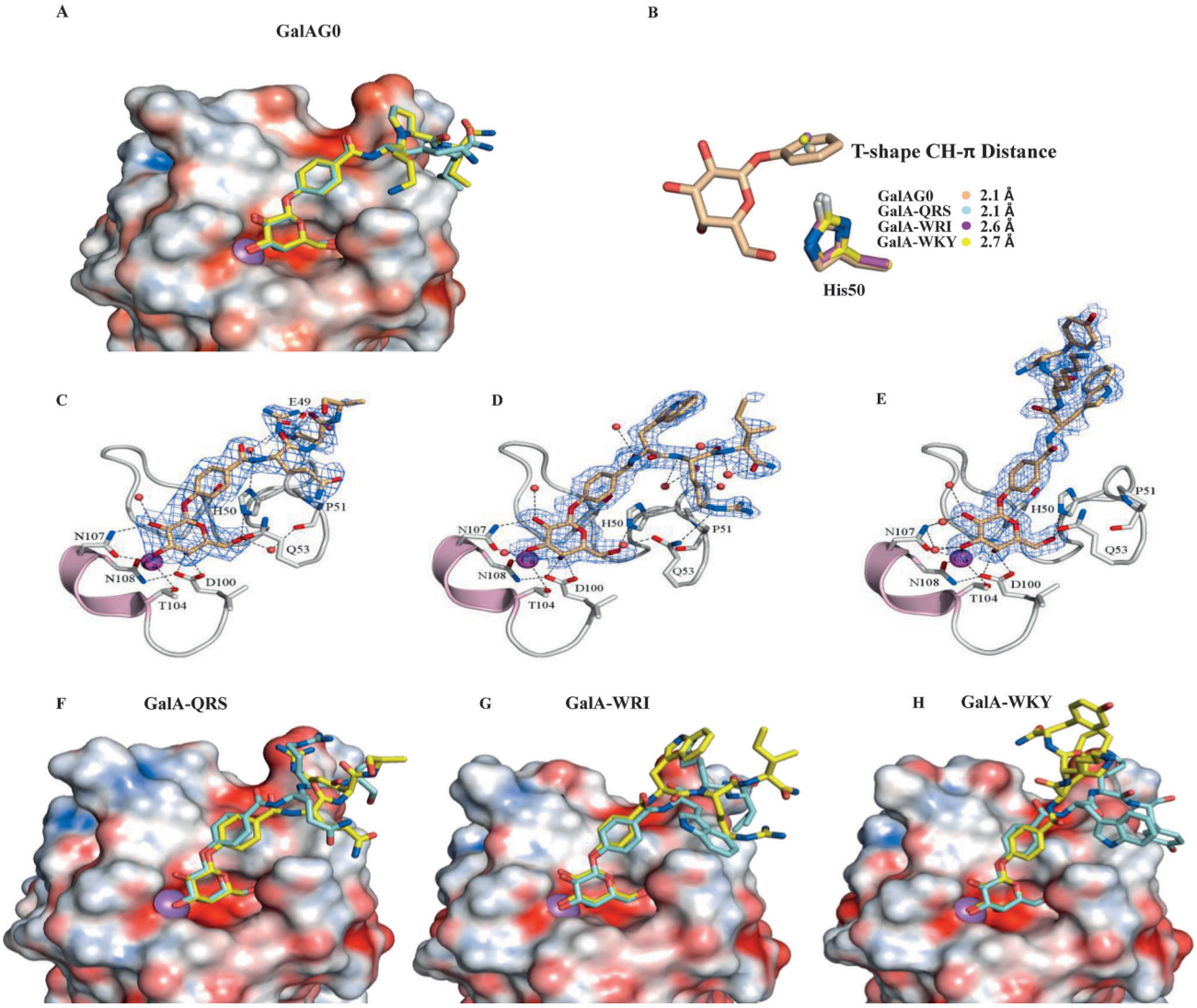

Figure 3. Structural and docking data for LecA complexes. A,F–H) Superimpositions of docked ligands (sky-blue colour sticks) with X-ray crystallographic ligands (yellow colour sticks); LecA is shown as a surface representation (C: white; N: blue; O: red), with the Ca^{++} ion indicated as a magenta sphere. The protein is depicted as a surface model collared according to electrostatic potentials, represented by a calculated charge from red (acidic residues; $-25\ K_bTe_c^{-1}$) to blue (basic residues; $+25\ K_bTe_c^{-1}$), as in the Adaptive Poisson–Boltzmann Solver (APBS) program in the PYMOL software. B) T-shaped CH–π distances in the solved crystal structures. C–E) Selected experimental poses observed in co-crystallised galactotripeptide–LecA complexes. The fit of the ligands to the electron-density map (contoured at 1 σ level) is shown. Noncovalent interactions between the ligand and the protein are shown by dotted lines. Atom labels: N: blue; O: red; Ca: magenta. All figures were generated by using the PyMol v1.3 software (www.PyMol.org). See also the structural formulae in Scheme 1.

Table 4. Synthesis and evaluation of the G2 galactopeptide dendrimers.

Compound	Sequence[a]	Mass ion calcd/obs	Yield [mg] ([%])	MIC[b] [μM]	r.p./n[c]	MBIC[d] [μM]	Disp.[e] [%]
G2QRS	(GalA-QRS)$_4$(*K*FKI)$_2$*K*HI	4043.4/4044	4.7 (1)	0.39	1700	34	45
G2KPY	(GalA-KPY)$_4$(*K*FKI)$_2$*K*HI	4111.7/4112	21.8 (4)	0.39	1700	30	80
G2KPW	(GalA-KPW)$_4$(*K*FKI)$_2$*K*HI	4203.8/4204	11.6 (2)	0.78	830	20	70

[a] Single letter codes for L-amino acids; branching lysine residues indicated by italics; GalA is 4-(β-galactosyloxy)benzoyl; the peptide C terminus is a carboxamide $CONH_2$ group. [b] MIC: minimum inhibition concentration in the hemagglutination assay with rabbit erythrocytes. See the Materials and Methods section for details. [c] r.p./n is the relative potency per galactosyl group ($n=4$), with the relative potency calculated as r.p.= MIC(galactose)/MIC(dendrimer). In these measurements, the MIC value for galactose was 2.5 mM and for **GalAG2** was 0.39 μM. [d] MBIC: minimum biofilm inhibition concentration. See the Materials and Methods for details. [e] Biofilm dispersal at 50 μM concentration.

sequence, yet compatible with multiple mutations. The possibility to retain and even improve the biofilm inhibition properties in several amino acid sequence variants of **GalAG2** suggests that it should be possible to fine-tune the dendrimer towards therapeutic use by adjusting the pharmacokinetic parameters in addition to the biofilm inhibition through variations of the amino acids.

Materials and Methods

Synthetic procedures and characterization of the various galactosylated tripeptides and peptide dendrimers are described in the Supporting Information.

In silico mutagenesis of glycopeptide ligands: Single-point mutant (SPM) and combined mutant (CM) ligands were generated in silico based on the native glycopeptide ligand sequence **GalAG0** (GalA-Lys-Pro-Leu-NH_2) by using the mutagenesis utility tool in the PyMol v1.3 software. Single-point mutations involved the mutation of each amino acid in the sequence with the 20 natural amino acids, with the β-phenyl-galactosyl part kept unaltered. This leads to 57 possible mutants in the SPM series (Figure S67 and Table S2 in the Supporting Information). Subsequently, the CMs were designed based on the best hits obtained from in silico docking and scoring of the SPMs (Table S3 in the Supporting Information).

Molecular docking and scoring:

Glycopeptide ligand geometry optimization: Glycopeptides with a core β-galactose phenyl group (GalA) with the amino acids P1, P2, and P3 in the corresponding positions were used for the molecular docking study. Subsequently, the built ligands were geometry optimized with the Macromodel v9.1 program (Schrodinger, LLC) by using the Optimized Potentials for Liquid Simulations–All Atom (OPLS-AA) force field[24]with the truncated Newton conjugate gradient protocol. Partial atomic charges were assigned according to the OPLS-AA force field.

Protein structure preparation and refinement: The X-ray crystal structure of lectin LecA from *P. aeruginosa* in complex with **GalAG0** (PDB ID: 3ZYB) obtained from the RCSB Protein Data Bank (PDB; http://www.rcsb.org) was used as the model for the protein structure in this study. Water molecules of crystallization were kept 5 Å around the co-crystallised ligand, and the protein was optimized for docking by using the protein preparation and refinement utility provided by Schrödinger LLC. Partial atomic charges were assigned according to the OPLS-AA force field.

Docking methodology and protocol: All docking calculations were performed by using the "Extra Precision" (XP) mode of the Glide program.[25] The accuracy of a docking procedure can be evaluated by determining how closely the lowest energy pose (binding conformation) predicted by the object scoring function resembles an experimental binding mode as determined by X-ray crystallography. In the present study, the Extra Precision Glide docking procedure was validated by removing the ligand from **GalAG0** from the co-crystallised LecA complex and re-docking into the binding site of LecA. A good agreement was observed between the localization of the inhibitor upon docking and from the crystal structure, that is, there were similar hydrogen-bonding interactions with N107, D100, Q53, and H50 and a similar Ca^{2+} coordination. The pairwise RMS value between the predicted conformation and the observed X-ray crystallographic conformation of **GalAG0** equalled 1.27 Å, a value that suggests the reliability of the docking program and the Glide parameter set in reproducing the experimentally observed binding mode for LecA from *P. aeruginosa*. The validated docking protocol was then used for docking the SPM and CM ligands into the crystal structure of the protein (Table S2 and S3 in the Supporting Information).

***P. aeruginosa* LecA expression and purification**: LecA was expressed and purified by affinity chromatography along an optimized protocol and in accordance with a previous report.[26] The plasmid pET25paIL was transformed into *Escherichia coli* BL21(DE3) cells. *E. coli* cells were grown in Luria–Bertani (LB) medium (6 L; tryptone (10 g), yeast extract (5 g), NaCl (5 g) in deionized water (1 L)) at 30 °C. When the culture had reached an optical density of 0.5–0.6 at 600 nm, isopropyl-β-D-thiogalactopyranoside (IPTG) was added to a final concentration of 0.1 mM. Cells were harvested after being left overnight with shaking at 220 rpm at 20 °C, washed, and resuspended in loading buffer (100 mL; 20 mM Tris–HCl, 100 μM $CaCl_2$, pH 7.5). The cells were broken by sonication. After centrifugation at 5000 rpm for 45 min, the supernatant was loaded onto an affinity chromatography column containing Sepharose 4B (250 mL). LecA was eluted with 0.2 M D-galactose in buffer (20 mM Tris–HCl, 100 μM $CaCl_2$, pH 7.5). The purified protein was extensively dialyzed against distilled water containing 2 μM $CaCl_2$ for 7 days and characterized by using SDS-PAGE and mass spectroscopy. Purified fractions of protein were lyophilized and kept at −20 °C.

Hemagglutination assay:

Erythrocyte preparation: Rabbit red cells (erythrocytes 50%; Biomerieux), separated from preservative by centrifugation (1500 rpm; 10 min), were washed three times with 0.9% NaCl solution (saline) and suspended to a concentration of 5% v/v in phosphate-buffered saline (PBS; 0.01 M; pH 7.4). The suspension was given papain treatment, which involves incubation of 9 volumes of the 5% cell suspension with 1 volume of the 1% w/v papain (crude preparation; Sigma) in 0.1% w/v L-cysteine solution at 37° for 30 min. The enzyme-treated cells were washed three times in PBS and then resuspended in PBS to a concentration of 5%.

LecA titration: In order to determine the lectin concentration needed to agglutinate the cells, decreasing amounts of LecA were incubated with the red blood cells. Serial twofold dilutions were made in the wells of a microtiter plate (96-well microtiter nontreated V-bottom plates; Nunc, Denmark). The twofold dilutions were made by adding buffer solution (50 μL) to all 24 wells and LecA solution (50 μL; 0.34 $mg\,mL^{-1}$) to the first well. A 50 μL volume was then transferred from the first well to the second. The second well was mixed and a 50 μL volume was transferred to the third well. This procedure was repeated until the 24th well. To each well, the red blood cell solution (50 μL; 5% in PBS) was added, and the mixture was incubated for 30 min at 4 °C. After this time, the plates were centrifuged for 30 s (1000 *g*), the wells were examined, and the minimum amount of LecA required to agglutinate the cell suspension was determined. This was then considered to be one HA unit. For the inhibition assay, an 8 HA unit LecA solution was made up.

Minimum inhibitory concentration determination: A 50 μL sample of each inhibitor examined was serially diluted with PBS (50 μL) in the microtiter plate to produce twofold dilutions (as described above). The inhibitor solutions were incubated with the 8 HA unit LecA solution (50 μL; conc. of LecA = 5.31 $\mu g\,mL^{-1}$) for 30 min at 4 °C. After this time, the erythrocytes in PBS suspension (50 μL; conc. = 5%) were added, and the wells were mixed and incubated for 1 h at room temperature. The plates were then centrifuged for 30 s (1000 *g*). Each test was performed in triplicate. The activity of the tested compounds was recorded as the minimum inhibitory concentration (MIC), which corresponded to the highest dilution that caused complete inhibition of hemagglutination (Figure S68–70 in the Supporting Information).

Biofilm formation on polystyrene microtiter plates: A modified version of the method described by Diggle et al. was employed.[5c] The 96-well, sterile, U-bottomed polystyrene microtiter plates (TPP, Switzerland) were prepared by adding sterile deionized water (200 μL) to the peripheral wells to decrease evaporation from the test wells. Aliquots of 180 μL of culture medium (10% w/v nutrient broth no. 2, Oxoid) containing the appropriate concentration of the test compound were added to the internal wells. For better solubility, **G2KPW** and **G2KPY** were dissolved in 10% w/v nutrient broth containing 5% v/v DMSO. An inoculum of *P. aeruginosa* strain PAO1 was prepared from a 5 mL overnight culture grown in LB broth. Aliquots (20 μL) of overnight cultures, prewashed in 10% w/v nutrient broth and normalized to an optical density at 600 nm (OD_{600}) of 1, were inoculated into the test wells. Plates were incubated in a humid environment for 25 h at 37 °C. Wells were washed with sterile deionized water (200 μL) before staining with 10% w/v nutrient broth (200 μL) containing 0.5 mM WST-8 and 20 μM phenazine ethosulfate for 3 h at 37 °C. Afterwards, the well supernatants were transferred to a polystyrene flat-bottomed 96-well plate (TPP, Switzerland), and the absorbance was measured at 450 nm with a plate reader (SpectraMax250 from Molecular Devices).

Isothermal titration calorimetry: Lyophilized LecA was dissolved in buffer (0.1 M Tris–base, pH 7.5, 25 mM $CaCl_2$). The protein concentration was checked by measurement of the absorbance at 280 nm by using a theoretical molarity extinction coefficient of $27600\,M^{-1}cm^{-1}$. Ligands were dissolved directly into the same buffer. ITC was performed with a iTC_{200} calorimeter (MicroCal Inc.). Titration was performed on 40 μM LecA in a 200 μL sample cell by using 1–2 μL injections of 1–1.5 mM ligand every

150 s at 25 °C. For reverse titrations performed on **GalA-KAL** and **GalA-WKY**, LecA was taken into the syringe at a concentration of 0.75 mM and the ligand was taken into the cell at concentrations ranging from 20–30 μM. The data were fitted with MicroCal Origin 8 software, according to standard procedures by using a single-site model. The change in free energy (ΔG) was calculated from the equation $\Delta G = \Delta H - T\Delta S$, in which T is the absolute temperature and ΔH and ΔS are the changes in enthalpy and entropy, respectively. Two independent titrations were performed for each ligand tested (Figure S73a and S73b in the Supporting Information).

X-ray crystallography: Co-crystallisation of **GalA-QRS**, **GalA-WRI**, and **GalA-WKY** with LecA was carried out by the sitting-drop method. In brief, lyophilized protein was dissolved in water (10 mg mL^{-1}) in the presence of salts (1 mM $CaCl_2$ and $MgCl_2$) and the respective galactoside ligand (0.5 mg mL^{-1}). In general, crystals were obtained within 3 d after mixing LecA solution (2 μL) with reservoir solution (2 μL) at 20 °C. Primary crystallization conditions included SaltRx I/II, respectively, from Hampton Research (Laguna Niguel, CA, USA). Nicely diffracting crystals were found in SaltRx II-24 (1.5 M lithium sulfate monohydrate), SaltRx I-5 (1.5 M ammonium chloride, 0.1 M Tris, pH 8.5), and SaltRx I-14 (3.2 M sodium chloride, 0.1 M Tris, pH 8.5), respectively.

LecA–galactoside crystals belong to space groups $C2$, $P2_12_12_1$, and $P4_322$ with the corresponding asymmetric units containing eight, four, and two monomers for **GalA-QRS**, **GalA-WRI**, and **GalA-WKY**, respectively. Further details on data collection statistics are given in Table 3. Crystals were cryocooled at 100 K after soaking them for as short a time as possible in 25% v/v glycerol in precipitant solution. All data were collected at the SLS synchrotron (Villigen, Switzerland) at beamline PX-III. Data were integrated and scaled with the X-ray detector software for processing single-crystal monochromatic diffraction data (XDS).[27] The structures of the co-crystallised ligands were solved by the molecular replacement technique with the Phaser program,[28] by using the monomeric structure (PDB code: 3ZYB) of the calcium- and galactose-containing LecA with galactose, calcium, and water molecules removed from the search probe. The molecular replacements gave clear solutions for all three ligand complexes, and the corresponding electron-density maps of the complexes showed clear features corresponding to the respective ligand. Automatic placement of water molecules was performed by using the ARP/wARP program.[29] Crystallographic refinements were carried out with the program phenix.refine from the PHENIX program package[30] and manual model building with COOT.[31]

Acknowledgements

This work was supported financially by the University of Berne, the Swiss National Science Foundation, and the COST Action CM1102 Multiglyconano. The authors thank Dr. A. Imberty for donation of the LecA expression plasmid and Prof. M. Sattler for support with ITC experiments. We gladly acknowledge beam time and support at the Swiss Light Source (PSI, Villigen, Switzerland).

[1] V. E. Wagner, B. H. Iglewski, *Clin. Rev. Allergy Immunol.* **2008**, *35*, 124–134.

[2] a) H.-P. Hauber, M. Schulz, A. Pforte, D. Mack, P. Zabel, U. Schumacher, *Int. J. Med. Sci.* **2008**, *5*, 371–376; b) M. N. Hurley, M. Camara, A. R. Smyth, *Eur. Respir. J.* **2012**, *40*, 1014–1023.

[3] G. Cioci, E. P. Mitchell, C. Gautier, M. Wimmerova, D. Sudakevitz, S. Perez, N. Gilboa-Garber, A. Imberty, *FEBS Lett.* **2003**, *555*, 297–301.

[4] a) E. Mitchell, C. Houles, D. Sudakevitz, M. Wimmerova, C. Gautier, S. Perez, A. M. Wu, N. Gilboa-Garber, A. Imberty, *Nat. Struct. Biol.* **2002**, *9*, 918–921; b) R. Loris, D. Tielker, K. E. Jaeger, L. Wyns, *J. Mol. Biol.* **2003**, *331*, 861–870.

[5] a) M. Mewe, D. Tielker, R. Schonberg, M. Schachner, K. E. Jaeger, U. Schumacher, *J. Laryngol. Otol.* **2005**, *119*, 595–599; b) D. Tielker, S. Hacker, R. Loris, M. Strathmann, J. Wingender, S. Wilhelm, F. Rosenau, K. E. Jaeger, *Microbiology* **2005**, *151*, 1313–1323; c) S. P. Diggle, R. E. Stacey, C. Dodd, M. Camara, P. Williams, K. Winzer, *Environ. Microbiol.* **2006**, *8*, 1095–1104.

[6] a) P. von Bismarck, R. Schneppenheim, U. Schumacher, *Klin. Paediatr.* **2001**, *213*, 285–287; b) C. Chemani, A. Imberty, S. de Bentzmann, M. Pierre, M. Wimmerova, B. P. Guery, K. Faure, *Infect. Immun.* **2009**, *77*, 2065–2075.

[7] A. Imberty, M. Wimmerova, E. P. Mitchell, N. Gilboa-Garber, *Microbes Infect.* **2004**, *6*, 221–228.

[8] a) S. Cecioni, R. Lalor, B. Blanchard, J. P. Praly, A. Imberty, S. E. Matthews, S. Vidal, *Chem. Eur. J.* **2009**, *15*, 13232–13240; b) I. Otsuka, B. Blanchard, R. Borsali, A. Imberty, T. Kakuchi, *ChemBioChem* **2010**, *11*, 2399–2408; c) S. Cecioni, S. Faure, U. Darbost, I. Bonnamour, H. Parrot-Lopez, O. Roy, C. Taillefumier, M. Wimmerova, J. P. Praly, A. Imberty, S. Vidal, *Chem. Eur. J.* **2011**, *17*, 2146–2159; d) Y. M. Chabre, D. Giguere, B. Blanchard, J. Rodrigue, S. Rocheleau, M. Neault, S. Rauthu, A. Papadopoulos, A. A. Arnold, A. Imberty, R. Roy, *Chem. Eur. J.* **2011**, *17*, 6545–6562; e) S. Cecioni, J. P. Praly, S. E. Matthews, M. Wimmerova, A. Imberty, S. Vidal, *Chem. Eur. J.* **2012**, *18*, 6250–6263.

[9] a) K. Marotte, C. Preville, C. Sabin, M. Moume-Pymbock, A. Imberty, R. Roy, *Org. Biomol. Chem.* **2007**, *5*, 2953–2961; b) F. Morvan, A. Meyer, A. Jochum, C. Sabin, Y. Chevolot, A. Imberty, J. P. Praly, J. J. Vasseur, E. Souteyrand, S. Vidal, *Bioconjugate Chem.* **2007**, *18*, 1637–1643; c) M. Andreini, M. Anderluh, A. Audfray, A. Bernardi, A. Imberty, *Carbohydr. Res.* **2010**, *345*, 1400–1407.

[10] B. Gerland, A. Goudot, G. Pourceau, A. Meyer, S. Vidal, E. Souteyrand, J. J. Vasseur, Y. Chevolot, F. Morvan, *J. Org. Chem.* **2012**, *77*, 7620–7626.

[11] a) A. Imberty, Y. M. Chabre, R. Roy, *Chem. Eur. J.* **2008**, *14*, 7490–7499; b) M. Brandl, M. S. Weiss, A. Jabs, J. Suhnel, R. Hilgenfeld, *J. Mol. Biol.* **2001**, *307*, 357–377; c) M. Levitt, M. F. Perutz, *J. Mol. Biol.* **1988**, *201*, 751–754; d) S. Tsuzuki, K. Honda, T. Uchimaru, M. Mikami, K. Tanabe, *J. Am. Chem. Soc.* **2000**, *122*, 3746–3753; e) M. Nishio, M. Hirota, Y. Umezawa, *CH/π Interaction. Evidence, Nature and Consequences*, Wiley-VCH, New York, **1988**.

[12] a) Y. C. Lee, R. T. Lee, *Acc. Chem. Res.* **1995**, *28*, 321–327; b) J. J. Lundquist, E. J. Toone, *Chem. Rev.* **2002**, *102*, 555–578.

[13] a) G. R. Newkome, C. N. Moorefield, F. Vögtle, *Dendrimers and Dendrons: Concepts, Syntheses, Applications*, Wiley-VCH, Weinheim, **2001**; b) N. Röckendorf, T. Lindhorst in *Glycodendrimers, Vol. 217* (Eds.: F. Vögtle, C. Schalley), Springer, Berlin, **2001**, pp. 201–238; c) R. Roy, *Trends Glycosci. Glycotechnol.* **2003**, *15*, 291–310; d) C. C. Lee, J. A. MacKay, J. M. Frechet, F. C. Szoka, *Nat. Biotechnol.* **2005**, *23*, 1517–1526; e) J. Kofoed, J. L. Reymond, *Curr. Opin. Chem. Biol.* **2005**, *9*, 656–664; f) R. J. Pieters, *Org. Biomol. Chem.* **2009**, *7*, 2013–2025; g) D. Astruc, E. Boisselier, C. Ornelas, *Chem. Rev.* **2010**, *110*, 1857–1959; h) E. C. Lee, B. H. Hong, J. Y. Lee, J. C. Kim, D. Kim, Y. Kim, P. Tarakeshwar, K. S. Kim, *J. Am. Chem. Soc.* **2005**, *127*, 4530–4537.

[14] E. M. Johansson, S. A. Crusz, E. Kolomiets, L. Buts, R. U. Kadam, M. Cacciarini, K. M. Bartels, S. P. Diggle, M. Camara, P. Williams, R. Loris, C. Nativi, F. Rosenau, K. E. Jaeger, T. Darbre, J. L. Reymond, *Chem. Biol.* **2008**, *15*, 1249–1257.

[15] R. U. Kadam, M. Bergmann, M. Hurley, D. Garg, M. Cacciarini, M. A. Swiderska, C. Nativi, M. Sattler, A. R. Smyth, P. Williams, M. Camara, A. Stocker, T. Darbre, J. L. Reymond, *Angew. Chem.* **2011**, *123*, 10819–10823; *Angew. Chem. Int. Ed.* **2011**, *50*, 10631–10635.

[16] a) J. L. Reymond, T. Darbre, *Org. Biomol. Chem.* **2012**, *10*, 1483–1492; b) J. L. Reymond, M. Bergmann, T. Darbre, *Chem. Soc. Rev.* **2013**, *42*, 4814–4822.

[17] E. M. V. Johansson, E. Kolomiets, F. Rosenau, K.-E. Jaeger, T. Darbre, J.-L. Reymond, *New J. Chem.* **2007**, *31*, 1291–1299.

[18] E. Kolomiets, E. M. Johansson, O. Renaudet, T. Darbre, J. L. Reymond, *Org. Lett.* **2007**, *9*, 1465–1468.

[19] a) E. Kolomiets, M. A. Swiderska, R. U. Kadam, E. M. Johansson, K. E. Jaeger, T. Darbre, J. L. Reymond, *ChemMedChem* **2009**, *4*, 562–569; b) E. M. V. Johansson, R. U. Kadam, G. Rispoli, S. A. Crusz, K.-M. Bartels, S. P. Diggle, M. Camara, P. Williams, K.-E.

Jaeger, T. Darbre, J.-L. Reymond, *MedChemComm* **2011**, *2*, 418–420.
[20] R. U. Kadam, D. Garg, J. Schwartz, R. Visini, M. Sattler, A. Stocker, T. Darbre, J. L. Reymond, *ACS Chem. Biol.* **2013**, *8*, 1925–1930
[21] a) N. W. Roehm, G. H. Rodgers, S. M. Hatfield, A. L. Glasebrook, *J. Immunol. Methods* **1991**, *142*, 257–265; b) M. Ishiyama, Y. Miyazono, K. Sasamoto, Y. Ohkura, K. Ueno, *Talanta* **1997**, *44*, 1299–1305; c) S. Stepanović, D. Vukovic, V. Hola, G. Di Bonaventura, S. Djukic, I. Cirkovic, F. Ruzicka, *APMIS* **2007**, *115*, 891–899; d) E. Peeters, H. J. Nelis, T. Coenye, *J. Microbiol. Methods* **2008**, *72*, 157–165.
[22] V. K. Dhir, C. E. Dodd, *Appl. Environ. Microbiol.* **1995**, *61*, 1731–1738.
[23] W. B. Turnbull, A. H. Daranas, *J. Am. Chem. Soc.* **2003**, *125*, 14859–14866.
[24] W. L. Jorgensen, D. S. Maxwell, J. Tirado-Rives, *J. Am. Chem. Soc.* **1996**, *118*, 11225–11236.
[25] a) R. A. Friesner, J. L. Banks, R. B. Murphy, T. A. Halgren, J. J. Klicic, D. T. Mainz, M. P. Repasky, E. H. Knoll, M. Shelley, J. K. Perry, D. E. Shaw, P. Francis, P. S. Shenkin, *J. Med. Chem.* **2004**, *47*, 1739–1749; b) T. A. Halgren, R. B. Murphy, R. A. Friesner, H. S. Beard, L. L. Frye, W. T. Pollard, J. L. Banks, *J. Med. Chem.* **2004**, *47*, 1750–1759.
[26] B. Blanchard, A. Nurisso, E. Hollville, C. Tetaud, J. Wiels, M. Pokorna, M. Wimmerova, A. Varrot, A. Imberty, *J. Mol. Biol.* **2008**, *383*, 837–853.
[27] W. Kabsch, *Acta Crystallogr. Sect. D Biol. Crystallogr.* **2010**, *66*, 125–132.
[28] A. J. McCoy, R. W. Grosse-Kunstleve, P. D. Adams, M. D. Winn, L. C. Storoni, R. J. Read, *J. Appl. Crystallogr.* **2007**, *40*, 658–674.
[29] A. Perrakis, R. Morris, V. S. Lamzin, *Nat. Struct. Biol.* **1999**, *6*, 458–463.
[30] P. D. Adams, P. V. Afonine, G. Bunkoczi, V. B. Chen, I. W. Davis, N. Echols, J. J. Headd, L. W. Hung, G. J. Kapral, R. W. Grosse-Kunstleve, A. J. McCoy, N. W. Moriarty, R. Oeffner, R. J. Read, D. C. Richardson, J. S. Richardson, T. C. Terwilliger, P. H. Zwart, *Acta Crystallogr. Sect. D Biol. Crystallogr.* **2010**, *66*, 213–221.
[31] P. Emsley, K. Cowtan, *Acta Crystallogr. Sect. D Biol. Crystallogr.* **2004**, *60*, 2126–2132.

Received: July 4, 2013
Revised: September 11, 2013
Published online: November 4, 2013

